Shock and Vibration 9 (2002) 19–27
IOS Press

Measuring strain response mode shapes with a continuous-scan LDV

Anthony B. Stanbridge*, Milena Martarelli and David J. Ewins
Department of Mechanical Engineering, Imperial College, London, UK

Abstract: A continuous-scan LDV is a convenient means for measuring the response mode shape (ODS) of a vibrating surface, particularly in view of the fact that the ODS is automatically derived as a spatial polynomial series. Second spatial derivatives of the deflection equations are therefore easily derived, and these should, in principle, give curvature equations from which, for a beam or plate of known cross-section, stresses and strains can be obtained directly. Unfortunately, the stress and strain distributions depend critically on higher terms in the original ODS series, which are not accurately measured. This problem can be avoided by a method described here, which enables accurate stress and strain distributions to be derived, from a straight-line LDV scan along a uniform beam, using only five terms in the mode-shape polynomial series. A similar technique could be applied to uniform plates but the analysis and the governing equations are rather more complicated.

Keywords: Laser Doppler vibrometer, scanning, vibration, stress, strain measurement

1. Introduction

The use of a continuous-scan laser Doppler vibrometer (CSLDV) for measuring the response mode shape of a structure's surface has been described elsewhere for straight-line [1], and rectangular [2], area scans. If the structure's vibration is sinusoidal at every point, the vibration measured during a continuous scan is amplitude modulated so that, in the frequency domain, there are components at the basic response frequency and at sidebands spaced symmetrically about it. These sideband data are easily processed to give the coefficients of a polynomial expression for the response mode shape.

Out-of-plane deflection mode-shape data may be sufficient to decide the viability of a design but, quite commonly, stress or strain data would be even more valuable, and these are, for simple beams and plates, functions of curvature, the second spatial differentials of the out-of-plane deflection. Spatial differentials may be obtained from finite difference equations, on the basis of arrays of discrete point response measurements, but the process is likely to be frustrated by random experimental errors. On the other hand, a CSLDV scan should, in principle, make the derivation of such differentials a trivial matter, because the response is directly available as an easily-differentiated polynomial series, and there are, at first sight, no random noise errors to contend with.

In practice, as we will see, with a CSLDV there are higher order terms in the response polynomial series that are small, have little influence on the deflection ODS, and are not measured accurately – indeed many of them are usually much too small to be measured at all. Although these do not much affect the deflection response shapes, they have a crucial influence on the curvature distribution, and so a CSLDV, used in this simple way, on the face of it, provides little improvement in accuracy over the discrete-point, finite difference method. However, a correction technique, proposed here for CSLDV analysis will, in some cases, overcome this problem completely.

2. Beam mode-shape measurement

If an LDV is scanned sinusoidaly along a straight line over a surface vibrating at a frequency ω, the LDV

*Corresponding author: Anthony Stanbridge, Mechanical Engineering Dept., Imperial College, Exhibition Road, London, UK, SW7 2BX. Fax: +44 207 584 1560; E-mail: a.stanbridge@ic.ac.uk.

ISSN 1070-9622/02/$8.00

output spectrum has a sideband structure, centred on ω, the sidebands being spaced at multiples of the scan frequency, Ω [1]. It is convenient for the analysis to assume the scan to be of amplitude $\pm$ 1, with zero at the scan mid-point, so that the point addressed is

$$x(t) = \cos \Omega t \tag{1}$$

The sideband structure is always, theoretically, symmetrical (although phase spectrum symmetry requires the signal sampling to be triggered suitably from the scan signal).

The beam vibration is assumed to follow a spatial polynomial series, defined along the line by:

$$\begin{aligned} v_z(x,t) = \sum_{n=0}^{p} \{ & V_{an} x^n \cos(\omega t + \alpha_n) \\ & + V_{bn} x^n \sin(\omega t + \alpha_n)\} \end{aligned} \tag{2}$$

Substituting for $x(t)$ from Eq. (1):

$$\begin{aligned} v_z(t) = \sum_{n} \{ & V_{an} \cos(\omega t + \alpha_n) \cos^n \Omega t \\ & + V_{bn} \sin(\omega t + \alpha_n) \cos^n \Omega t\} \end{aligned} \tag{3}$$

When Eq. (3) is expanded out, multiple terms arise at frequencies $(\omega \pm n\Omega)$. The in-phase (real) and quadrature (imaginary) parts of the upper and lower sidebands are equal, i.e.

$$\begin{aligned} v_z(t) = \sum_{n=-p}^{+p} \{ & S_{an}[\cos(\omega - n\Omega)t \\ & + \cos(\omega + n\Omega)t] \\ & + S_{bn}[\sin(\omega - n\Omega)t + \sin(\omega + n\Omega)t]\} \end{aligned} \tag{4}$$

After some manipulation, it can be shown that the sideband coefficients, $\{S_a\}$ and $\{S_b\}$ in Eq. (4), are related to the ODS polynomial coefficients, $\{V_a\}$ and $\{V_b\}$ in Eq. (3), by a simple matrix transform:

$$\{V_a\} = [T]\{S_a\} \text{ and } \{V_b\} = [T]\{Sb\} \tag{5}$$

Suffixes a and b are used for real (in-phase) and imaginary (quadrature) mode-shape components, respectively. The matrix $[T]$ has been derived explicitly elsewhere [1].

Real and imaginary components of the ODS depend on a reference vector, often the input force signal, for their definition. If, however, one of the larger ODS coefficients is assumed real, and used as the reference, the extent or absence of complexity in the ODS is more easily seen; in many cases the ODS will be entirely real and only one of the Eq. (5) need then be employed.

Equation (5) may also be used in reverse, so that, if a polynomial series has been established for a particular ODS or natural mode shape, the sideband pattern to be expected from a relevant LDV scan is given by:

$$\{S\} = [T]^{-1}\{V\} \tag{6}$$

2.1. Curvature analysis

Suppose that a CSLDV is scanned along a length $\pm L$ of a beam, vibrating at a frequency ω. Then, as described above, the ODS may be obtained as two series, for real and imaginary components, each of the form

$$\begin{aligned} V = V_0 + V_1 \frac{x}{L} + V_2 \left(\frac{x}{L}\right)^2 + V_3 \left(\frac{x}{L}\right)^3 \\ + V_4 \left(\frac{x}{L}\right)^4 + \text{etc.} \end{aligned} \tag{7}$$

For a simple Euler beam, the surface strain at a point is $z\frac{\partial^2 y}{\partial x^2}$, z being the distance between the surface and the bending neutral axis, and y the displacement at a point x. The strain produced by the ODS is $z\frac{\partial^2 V}{\partial x^2}$ and the corresponding stress is simply $Ez\frac{\partial^2 V}{\partial x^2}$, where E is Young's modulus, and V stands for either the real or the imaginary component of the ODS.

The bending moment at a point x_1 is

$$M_1 = -EI \left(\frac{\partial^2 V}{\partial x^2}\right)_{x=x_1}, \tag{8}$$

I being the second moment of area for the beam cross-section.

i.e.

$$\begin{aligned} M_1 = -EI \Bigg(& 2\frac{V_2}{L^2} + 6\frac{V_3 x_1}{L^3} + 12\frac{V_4 x_1^2}{L^4} \\ & + 20\frac{V_5 x_1^3}{L^5} + 30\frac{V_6 x_1^4}{L^6} + 42\frac{V_7 x_1^5}{L^7} + \text{etc.}\Bigg) \end{aligned} \tag{9}$$

2.2. Correction of ODS coefficients

Scanned LDV measurements are, of course, not free from error and it is obvious from Eq. (9) that inaccuracies in higher-order polynomial series terms have a far greater impact on the curvature, stress and strain than they do on out-of-plane displacement. It is, however, possible to correct higher order series coefficients when the underlying form of the stress expression is known, as it is for a uniform beam, because the ODS is, in fact, controlled by only a limited number of parameters: five in this particular case.

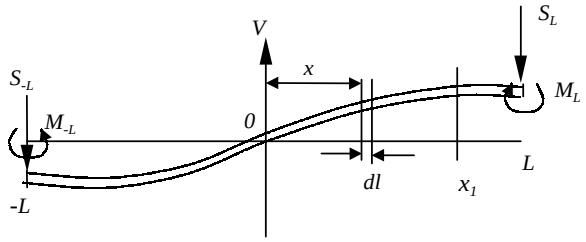

Fig. 1. Deflected form of a simple beam.

If the scanned part of the beam, length $\pm L$, is uniform, straight and free, i.e. there are no other constraints, added masses, etc. over this length, the bending moment can also be expressed (Fig. 1) in terms of the moment and shear force at the left-hand end, and the inertial moments due to vibration. i.e. the bending moment M_1, at a point, distance x_1 from the centre is:

$$M_1 = M_{-L} + S_{-L}(x_1 + L) - \int_{-L}^{x_1} \rho V \omega^2 (x_1 - x) dx \tag{10}$$

where ρ is the line density of the beam, in kg per m length.

By expanding V using Eq. (7), the integral in Eq. (10) is easily evaluated to give a series in x_1^n and, equating the resulting terms in x_1^2 and above to those in Eq. (9), one obtains:

$$\begin{aligned} \frac{\rho}{EI} &= \frac{24V_4}{\omega^2 L^4 V_0} = \frac{120V_5}{\omega^2 L^4 V_1} \\ &= \frac{360V_6}{\omega^2 L^4 V_2} = \frac{840V_7}{\omega^2 L^4 V_3} \\ &= \frac{1680V_8}{\omega^2 L^4 V_4} = \frac{3024V_9}{\omega^2 L^4 V_5} = \ldots \text{ etc.} \end{aligned} \tag{11}$$

(ω is the vibration frequency in rads/s, L is the (half) scan length, ρ is the line density, E the Young's modulus, I the area second moment, and V_n the nth polynomial coefficient.)

And, directly from Eq. (11),

$$\begin{aligned} V_5 &= \frac{V_1 V_4}{5V_0},\ V_6 = \frac{V_2 V_4}{15V_0},\ V_7 = \frac{V_3 V_4}{35V_0}, \\ V_8 &= \frac{V_4^2}{70V_0},\ V_9 = \frac{V_1 V_4^2}{630V_0^2}, \\ V_{10} &= \frac{V_2 V_4^2}{3150V_0^2},\ V_{11} = \frac{V_3 V_4^2}{11550V_0^2}, \\ V_{12} &= \frac{V_4^3}{34650V_0^2}, \text{ etc.} \end{aligned} \tag{12}$$

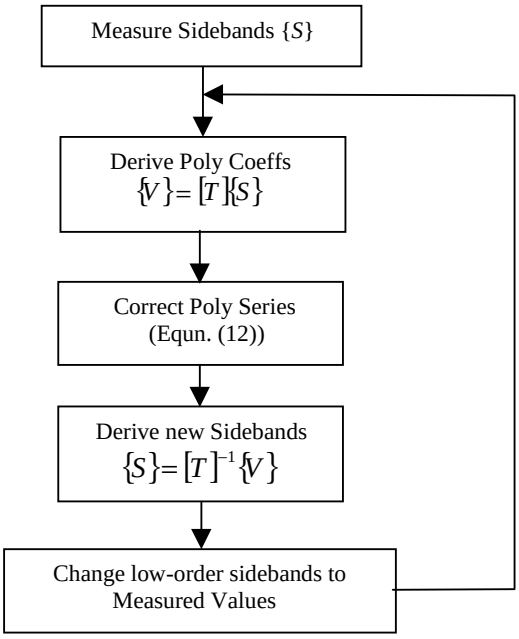

Fig. 2. Flow diagram for iterative improvement of measured uniform-beam LDV sine-scan data.

In principle therefore, if just five polynomial coefficients are known, all others may be derived, provided that the section of beam being scanned may be assumed to have a uniform cross-section. Note also that Eq. (11) may be used to derive a value for $\frac{\rho}{EI}$ which may be applied to mode shapes which are acquired at any other vibration frequency.

Equation (12) can also be used to extend sets of experimental polynomial coefficients, thus providing a basis for more exact curvature expressions. In fact, an iterative procedure is appropriate, because the extended set of polynomial coefficients can then be used to compute a corresponding set of sideband coefficients which will be different from the original measured values. This procedure is outlined in the flow diagram, Fig. 2. When convergence is achieved, the set of polynomial coefficients conforms to Eq (12), and the lower sidebands, derived by using Eq. (6), are the same as the measured values.

Some applications are described below.

2.3. ODS Scaling

If quantitative stress and strain levels are required, it should be noted that an LDV inherently measures the vibration velocity of the point addressed, rather than its displacement. The displacement, w_Z, is given by a modification of Eq. (2), as $w_z(x,t) =$

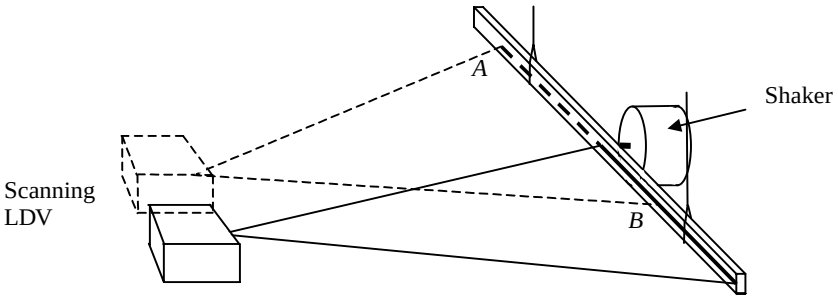

Fig. 3. Test set-up for LDV scan on a simple beam.

Table 1
Half-beam scan CSLDV data, Mode 3

1 Order	2 Measured sidebands	3 Initial deflection poly. coeffs.	4 Initial curvature poly. coeffs.	5 Iterated deflection poly. coeffs.	6 Iterated curvature poly. coeffs.	7 Sidebands (from column 5)
0	61.4	−170.9	1341	−172.2	1392	61.40
1	−5.30	−181.0	1736	−183.9	1721	−5.30
2	100.0	670.7	−3702	696.2	−4599	100.0
3	25.84	289.4	−2324	286.8	−1637	25.84
4	−15.48	−308.5	1210	−383.3	3099	−15.48
5	−1.04	−116.2	1989	−81.86	766	−1.65
6	0.63	40.32	0	103.3	−682	1.28
7	0.37	47.36	0	18.24	−104	0.12
8	0	0	0	−12.19	99	−0.038
9	0	0	0	−1.45	14	−0.002
10	0	0	0	1.10	−7	0.0009
11	0	0	0	0.123	−1	0.0001
12	0	0	0	−0.055	0	0
13	0	0	0	−0.0044	0	0
14	0	0	0	0.0024	0	0
15	0	0	0	0.0002	0	0

$$\sum_{n=0}^{p}\left(\frac{V_{an}}{\omega}x^n\sin(\omega t+\alpha_n)-\frac{V_{bn}}{\omega}x^n\cos(\omega t+\alpha_n)\right),$$

and this scaling applies equally to the curvature, stress and strain distributions, if obtained directly from LDV (velocity) signals. This modification is unnecessary if, as is often the case, only the *distribution* of stress and strain is required; the measured sideband amplitudes may then be used directly.

3. Experimental investigation

To check on the accuracy of the curvature and deflection measurements for straight-line CSLDV scans, measurements have been made on a simple, free-free steel beam, 32 mm wide, 10 mm thick and 950 mm long, as illustrated in Fig. 3.

The beam was supported by thin cords and excited by a small shaker attached to its centre, as shown. Excitation at a natural frequency was ensured by monitoring the input force with a piezoelectric force gauge, the frequency being adjusted until the force signal was minimal. At this condition, the response could be virtually guaranteed to be in a pure natural mode-shape. Two scan positions were employed, as indicated in Fig. 3, one between the mid-point and one end, the other between points A and B in the Figure.

Table 1 lists sideband amplitudes and polynomial coefficients, derived from the CSLDV data, for excitation at the third mode natural frequency, 313.6 Hz, with a scan over the right-hand half of the beam. The response mode shape, plotted from this 7th order polynomial (column 3 in Table 1), is compared with the theoretical mode-shape in the left-hand side of Fig. 4. The two curves are gratifyingly similar. (The theoretical Mode 3 deflection mode shape is of the form:

$$\begin{aligned} y = {} & (\cos 2.749(x+3)+\cosh 2.749(x+3)) \\ & -0.9999665(\sin 2.749(x+3) \\ & +\sinh 2.749(x+3)), \end{aligned} \tag{13}$$

an equation derived from standard theory [3].)

On taking second differentials, the measured polynomial inevitably gave a 5th order polynomial, with the coefficients listed in Table 1, column 4. The resulting fifth-order curve shows considerable error from the theoretical solution (dashed line on right-hand side of Fig. 4). A corrected polynomial series, extended and iterated as described above, is included in Table 1 column 5, and the second differential curvature series coefficients in column 6. The curvature distribution, plotted from the column 6 coefficients, is greatly improved, as indicated by the dotted line on the right hand side of Fig. 4.

100 iterations were applied to ensure convergence on an optimum solution. The sidebands equivalent to this final estimate were obtained using Eq. (6), and are listed in Table 1, column 7, for comparison with the original measured sidebands (column 2). It may be noted that the first five of these are, as they should be, identical with the original measurements. These five sidebands are the only data used to derive the curvature distribution in this procedure; the accuracy therefore depends on the accuracy with which they were measured initially.

Lest the half-span scan be thought to be a special case, Fig. 5 illustrates a similar measurement with a scan over a different region of the beam, A–B in Fig. 3. Again, the uncorrected deflection mode shape appears to be quite satisfactory, but there are considerable errors in the curvature distribution, which are removed by the iterative series-extension process.

3.1. A low-order mode – a special case

A similar process has been applied, using a half-span scan, with the beam vibrating in its lowest free-free bending mode, at 57.9 Hz. The theoretical Mode 1 deflection mode shape is:

$$\begin{aligned} y = {} & (\cos 1.1825(x+3) + \cosh 1.1825(x+3)) \\ & -0.9825(\sin 1.1825(x+3) \\ & + \sinh 1.1825(x+3)) \end{aligned} \tag{14}$$

Measured sideband amplitudes and derived polynomial series coefficients are listed in Table 2.

As before (Fig. 6) the approximation to the deflection response mode shape is quite satisfactory, but the derived curvature is poor. In fact, since the experimental measurement produced a cubic equation for the mode-shape, only two terms remain after double differentiation, and the curvature distribution is, on this basis, necessarily a straight line, as it would be for a static deflection situation in which there is no dynamic, inertia loading.

The procedure used to improve the curvature measurement for Mode 3 cannot be directly employed in this case because only four polynomial terms were obtained from the scan measurement, and five are needed if Eq. (12) are to be used. However, the Mode 3 results were used, with Eq. (11), to establish a value for $\frac{L^4\rho}{EI}$. Specifically, for Mode 3, $24\frac{V_4}{V_0} = 53.32$ and, therefore, for Mode 1, $24\frac{V_4}{V_0} = 53.32 \times \frac{57.9^2}{313.6^2} = 1.8177,\ V_4 = \frac{1.8177V_0}{24}$ and $V_5 = \frac{1.8177V_1}{5\times 24}$.

The polynomial series could now be extended and iterated as before.

The final result, although a considerable improvement, is not as good as for the Mode 3 results. The final data can, of course, be no better than the initial sideband data.

3.2. Identification of beam section properties

Equation (11) may be used to check the section properties of a simple beam, experimentally. In the case-study covered in this paper these are easily calculated, but in other situations, with built-up beams, or with beams of complicated cross section, density and second moments of area may be less certain and there may be some merit in being able to check them by an experimental procedure.

For the test beam, the line density, ρ, was 2.5 kg/m and the second moment of area, I, was 2.683×10^{-9} m^4, based on an assumed density of 7800 kg/m^3 and measured dimensions. These, together with an assumed Young's modulus of 207 GPa, give an estimated value of ρ/EI of 0.00450 s^{2}m^{-4}.

Each ratio in Eq. (11) should give the same value for ρ/EI when based on iterated polynomial deflection coefficients, because this is, effectively, the convergence criterion for the iteration. The data in Table 1, with a (half) scan length of 0.2375 m, and a frequency $\omega = 2\pi \times 313.6$ Hz, give a value of ρ/EI of 0.00433 s^{2}m^{-4}. The scan data on which Fig. 5 is based gave $\rho/EI = 0.00451$. It may be noted that a previous attempt [4], to identify beam properties in this way was rather unsuccessful because no iteration process was employed and the polynomial coefficients were hence not sufficiently accurately determined.

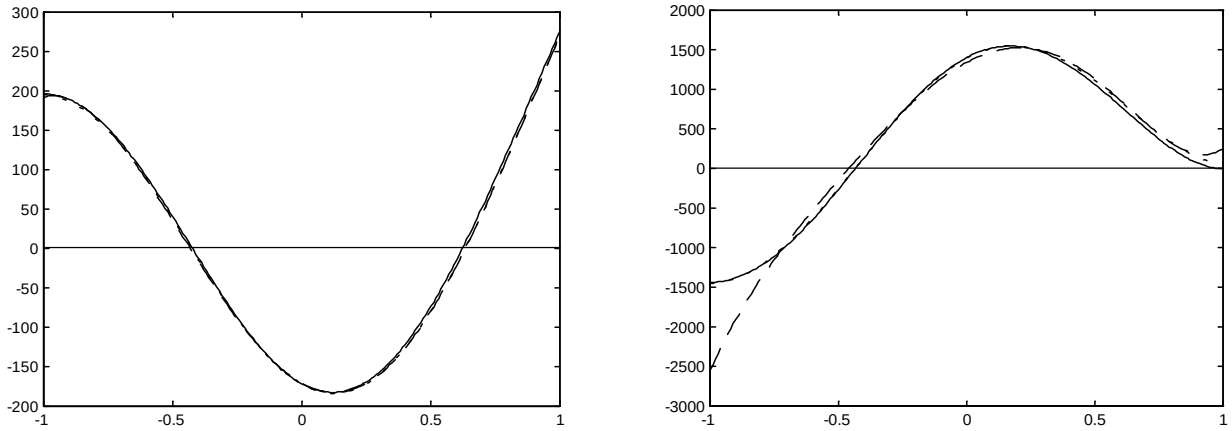

Fig. 4. Mode 3 deflected form (LHS) and curvature (RHS) for a Free-Free Beam. LDV scan between the centre and the tip: Theoretical (full line), Initial measurement (dashes), Final iteration (dotted).

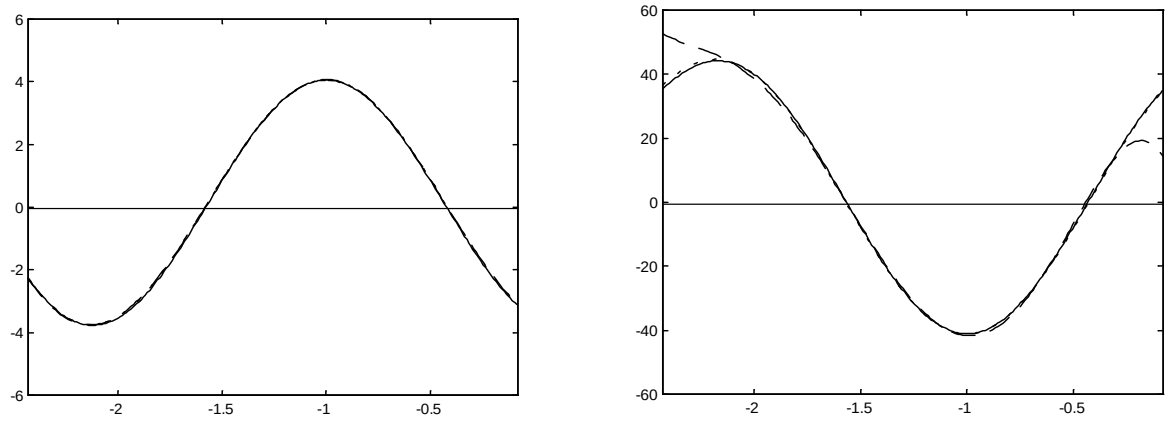

Fig. 5. Mode 3 deflected form (LHS) and curvature (RHS) for a Free-Free Beam. LDV scan A–B: Theoretical (full line), Initial measurement (dashes), Final iteration (dotted).

Table 2
Half-beam scan CSLDV data, Mode 1

1 Order	2 Measured sidebands	3 Initial deflection poly. coeffs.	4 Initial curvature poly. coeffs.	5 Iterated deflection poly. coeffs.	6 Iterated curvature poly. coeffs.	7 Sidebands (from column 5)
0	12.71	−22.6	141.0	−22.7	143.9	12.71
1	100.0	219.4	−155.5	220.5	−180.1	100.0
2	17.64	70.6	0	71.94	−20.6	17.64
3	−3.24	−25.9	0	−30.0	66.8	−3.24
4	0	0	0	−1.72	10.8	−0.074
5	0	0	0	3.34	−2.7	0.101
6	0	0	0	0.363	−0.1	0.0056
7	0	0	0	−0.065	0.1	−0.0005
8	0	0	0	−0.0019	0	0
9	0	0	0	0.002	0	0

4. Plate vibration

The basic principle described above can, in principle, be extended to plate vibration. A CSLDV rectangular area scan will give ODS deflection coefficients $V_{n,m}$ for a vibration velocity polynomial series of the form:

$$v_z(x,y,t) = \sum \{V_{an,m} x^n y^m \cos(\omega t + \alpha_n)$$

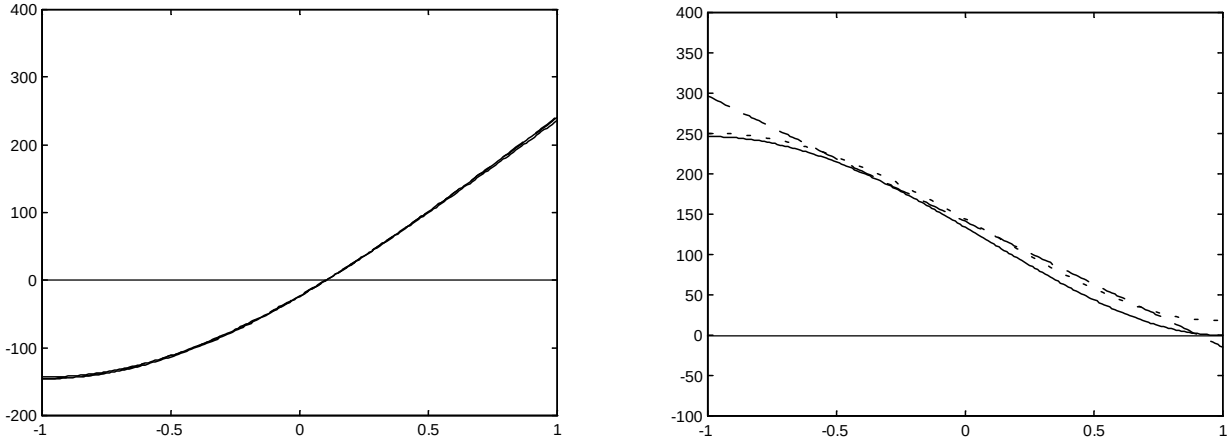

Fig. 6. Mode 1 deflected form (LHS) and curvature (RHS) for a Free-Free Beam. LDV scan between the centre and the tip: Theoretical (full line), Initial measurement (dashes), Final iteration (dotted).

$$+V_{bn,m}x^n y^m \sin(\omega t + \alpha_n)\}$$

Real and imaginary ODS polynomial coefficients for the deflection $w(x,y,t)$, are $\frac{V_{an,m}}{\omega}$ and $-\frac{V_{bn,m}}{\omega}$.

From classical theory [5], the normal strains in x- and y-direction at the surface of an isotropic plate are:

$$\varepsilon_x = z\frac{\partial^2 w}{\partial x^2} \quad \varepsilon_y = z\frac{\partial^2 w}{\partial y^2}$$

and the shear strain is: $\gamma_{xy} = 2z\dfrac{\partial^2 w}{\partial x \partial y}$

z being the plate half-thickness. If the scan lengths are $\pm L_X$ in the x direction, and $\pm L_Y$ in the y direction, then

$$\begin{aligned}
\frac{\partial^2 w}{\partial x^2} &= \frac{1}{\omega^2 L_X^2}\sum_{n,m} n(n-1)V_{n,m} \\
&\quad \left(\frac{x}{L_X}\right)^{n-2}\left(\frac{y}{L_Y}\right)^{m} \\
\frac{\partial^2 w}{\partial y^2} &= \frac{1}{\omega^2 L_Y^2}\sum_{n,m} m(m-1)V_{n,m} \\
&\quad \left(\frac{x}{L_X}\right)^{n}\left(\frac{y}{L_Y}\right)^{m-2} \\
\frac{\partial^2 w}{\partial x \partial y} &= \frac{1}{\omega^2 L_X L_Y}\sum_{n,m} nmV_{n,m} \\
&\quad \left(\frac{x}{L_X}\right)^{n-1}\left(\frac{y}{L_Y}\right)^{m-1}
\end{aligned} \tag{15}$$

where x and y define the position on the plate, from the centre of the scan. The strains at x, y are therefore:

$$\begin{aligned}
\varepsilon_x &= \frac{z}{\omega L_X^2}\sum_{n,m} n(n-1)V_{n,m} \\
&\quad \left(\frac{x}{L_X}\right)^{n-2}\left(\frac{y}{L_Y}\right)^{m} \\
\varepsilon_y &= \frac{z}{\omega L_Y^2}\sum_{n,m} m(m-1)V_{n,m} \\
&\quad \left(\frac{x}{L_X}\right)^{n}\left(\frac{y}{L_Y}\right)^{m-2} \\
\gamma_{xy} &= \frac{2z}{\omega L_X L_Y}\sum_{n,m} nmV_{n,m} \\
&\quad \left(\frac{x}{L_X}\right)^{n-1}\left(\frac{y}{L_Y}\right)^{m-1}
\end{aligned} \tag{16}$$

and the stresses are:

$$\begin{aligned}
\sigma_x &= \frac{E}{1-\nu^2}(\varepsilon_x + \nu\varepsilon_y), \\
\sigma_y &= \frac{E}{1-\nu^2}(\varepsilon_x + \nu\varepsilon_x), \\
\tau_{xy} &= \frac{E}{2(1+\nu)}\gamma_{xy}
\end{aligned} \tag{17}$$

E is the Young's modulus and ν the Poisson's ratio.

The stresses and strains can thus all be computed quite straight-forwardly from the measured polynomial series for the deflection, just as they can for a simple beam, but with the same reservation that the series is almost certainly inaccurate, especially the higher-order terms.

The augmentation and iteration process, described in 2.2 for a uniform beam, can be adapted to uniform-thickness plates. Proceeding as before, the bending

moment intensities at point x, y in a plane, parallel to the x- and y axes are

$$M_x = -D\left(\frac{\partial^2 w}{\partial x^2} + \nu\frac{\partial^2 w}{\partial y^2}\right) \text{ and}$$

$$M_y = -D\left(\frac{\partial^2 w}{\partial y^2} + \nu\frac{\partial^2 w}{\partial x^2}\right).$$

and the twisting moment is:

$$M_{xy} = -D(1-\nu)\frac{\partial^2 w}{\partial x \partial y} \tag{18}$$

Where $D = \frac{2Ez^3}{3(1-\nu^2)}$ is the flexural rigidity.

Equations (18) are analagous to Eq. (8) for a simple beam, and can be expanded in the same way, using the polynomial coefficients. Moment intensity equations at the point x, y, similar to Eq. (10) can be derived in terms of the vibratory inertia loading:

$$\begin{aligned} &M_{y1} + M_{x1y1} \\ &= M_{-Ly} + S_{-Ly}(y_1 + L_y) \\ &\quad - \int_{-L_y}^{ly1} 2\omega^2 \rho w L_x (y_1 - y) dy \text{ and} \\ &M_{x1} + M_{x1y1} \\ &= M_{-Lx} + S_{-Lx}(x_1 + L_x) \\ &\quad - \int_{-L_x}^{lx1} 2\omega^2 \rho w L_y (x_1 - x) dx \end{aligned} \tag{19}$$

Equations (18) and (19) can be evaluated and solved to give the fifth-order ODS polynomial terms, and above, in terms of the lower terms $V_{0,0}$ to $V_{4,4}$. The formulae are more complicated than those in Eq. 12, for beams. As examples:

$$\begin{aligned} V_{0,5} = \frac{-1}{60V_{0,0}}&(12V_{0,0}V_{1,4}(1-\nu) \\ &+6\nu V_{0,0}V_{2,3} - 3V_{0,1}V_{1,3} \\ &-2\nu V_{0,1}V_{2,2} + 3\nu V_{0,1}V_{1,3} \\ &-12V_{0,1}V_{0,4}) \\ V_{1,5} = \frac{-1}{60V_{0,0}}&(24V_{0,0}V_{2,4}(1-\nu) \\ &+18\nu V_{0,0}V_{3,3} - 3V_{1,1}V_{1,3} \\ &-2\nu V_{1,1}V_{2,2} + 3\nu V_{1,1}V_{1,3} \\ &-12V_{1,1}V_{0,4}) \end{aligned} \tag{20}$$

The iteration outlined in Fig. 2 may be used for plates as well as beams, though the arithmetic is obviously more extensive.

The practical need for a stress distribution derivation process is probably less for plates than it is for beams. There are, arguably, relatively few structures in which there are uniform plates, subject to vibration, with clear areas devoid of connections to other components, stiffening ribs, etc., which would invalidate the analysis assumptions. On the other hand, free uniform beams are relatively frequently employed as components in structural assemblies.

5. Concluding comments

Stress and strain distributions due to sinusoidal bending vibration of beams and plates can be derived from second spatial derivatives of displacement ODSs and this process is, in principle, particularly simple if the ODS mode shape is available as a spatial polynomial expression – which is the case if a CSLDV is used.

This possibility has been explored for the case of a uniform free-free beam. A straight-line sine-scan LDV was used. LDV output spectrum data: amplitude and phase at the centre frequency and at sideband pairs, were processed to give polynomial coefficients. Unfortunately, higher terms which are too small to be measured have a crucial influence on stress and strain distributions, particularly in the outer 25% of the scanned line, which is often the most highly stressed part of the beam.

The deflection polynomial coefficients for a clear span of a uniform beam are linked by simple relationships, and an iterative process has been devised, on this basis, which converges on a polynomial series that gives a much-improved curvature distribution. (The final result can never, of course, be better than that dictated by the accuracy of the original measurements.) If the correction process is not applied, deflection ODSs may be measured with good accuracy, but curvature, bending moment, stress or strain distributions, derived from second differentials, will never be reliable. The iterative process described here is applicable only to bending modes of straight, uniform, slender beams, to which Euler beam theory applies. It is also a requirement that the beam segment scanned is free, that is to say, there must be no external forces due to attached structures, within the scanned line. The beam may, however, be constrained in any way at the ends of the scanned line.

The iteration technique fails if the mode-shape approximates to a static deflection (cubic) curve. How-

ever, data from another ODS can be used, in this case, to improve the estimate of curvature distribution.

A similar, but more complicated, processing technique can also be applied to vibration modes of flat uniform plates.

Acknowledgements

The authors gratefully acknowledge the support given by the BRITE EURAM "VALSE", project no. BE97-4126, to this work. We would also like to thank all the other partners in the project for their interest and cooperation.

References

[1] A.B. Stanbridge and D.J. Ewins, Modal testing using a scanning laser Doppler vibrometer, *Mechanical Systems and Signal Processing* **13**(2) (1999), 255–270.

[2] A.B. Stanbridge, M. Martarelli and D.J. Ewins, Measuring area vibration mode shapes with a continuous-scan LDV. *Vibration Measurements by Laser Techniques* (4), *Ancona, Proc. SPIE* **4072** (2000), 176–183.

[3] S.P. Timoshenko, D.H. Young and W.W. Weaver, *Vibration Problems in Engineering,* (4th ed.), Wiley, New York, 1974.

[4] A.B. Stanbridge and D.J. Ewins, Scanning laser Doppler vibrometer data for vibrating beam system identification, *IMAC* **16** (1998), 1498–1504.

[5] A.W. Leissa, Vibration of plates: NASA 1969; SP-160, 1969.